Development of an alpha-particle imaging detector based on a low radioactive micro-time-projection chamber

H. Ito[a*], T. Hashimoto[a], K. Miuchi[a], K. Kobayashi[b,c], Y. Takeuchi[a,c], K. D. Nakamura[a], T. Ikeda[a], and H. Ishiura[a]

[a] *Kobe University, Kobe, Hyogo 657-8501, Japan.*

[b] *Institute for Cosmic Ray Research (ICRR), the University of Tokyo, Kashiwa, Chiba 277-8582 Japan.*

[c] *Kavli Institute for the Physics and Mathematics of the Universe (WPI), The University of Tokyo Institutes for Advanced Study, University of Tokyo, Kashiwa, Chiba 277-8583, Japan.*

Abstract

An important issue for rare-event-search experiments, such as the search for dark matter or neutrinoless double beta decay, is to reduce radioactivity of the detector material and the experimental environment. The selection of materials with low radioactive impurity, such as isotopes in the uranium and thorium chains, requires a precise measurement of surface radioactivity. An alpha-particle detector has been developed based on a gaseous micro-time-projection chamber. A low-α μ-PIC with reduced alpha-emission background was installed in the detector. The detector offers the advantage of position sensitivity, which allows the alpha-particle contamination of the sample to be imaged and the background to be measured at the same time. The detector performance was measured by using an alpha-particle source. The measurement with a sample was also demonstrated and the sensitivity is discussed.

Keywords: Alpha-particle detector, Position sensitivity, Time projection chamber, μ-PIC, Low background

1. Introduction

Approximately 27% of the universe is dominated by nonbarionic matter, called dark matter. Although many experimental groups have been searching for dark matter, no direct detection of dark matter has yet been reported. Typical experiments that search for dark matter are performed by using massive, low-background detectors. Although the DAMA group has observed the annual modulation with a significance of 9.3σ as the dark matter contribution [1], other groups such as XENON1T [2] and LUX [3] did not reproduced the signal. Meanwhile, a direction-sensitive method has been focused because of an expected clear anisotropic signal due to the motion of the solar system in the galaxy [4]. The NEWAGE group precedes a three-dimensionally sensitive dark matter search with a micro-time-projection chamber (micro-TPC) and the main background is surface alpha particles from ^{238}U and ^{232}Th in the detector material or in the μ-PIC [5].

Neutrinoless double beta ($0\nu\beta\beta$) decay is a lepton-number-violating process, which suggests the neutrino as a Majorana particle (it is its own antiparticle) and provides the absolute neutrino mass. The GERDA [6] and KamLAND-Zen [7] groups recorded a lower-limit half-life over 10^{25} yr at 90%CL by using ^{76}Ge and ^{136}Xe, respectively, and the $0\nu\beta\beta$ decay has yet to be observed. Conversely, a tracking system for two electrons provides strong evidence of the $0\nu\beta\beta$ decay process. The NEMO3 group precedes the measurement with at $T_{1/2} > 2.5 \times 10^{23}$ yr (90%CL) for ^{82}Se [8], and $T_{1/2} > (1.1 - 3.2) \times 10^{21}$ yr (90%CL) for ^{150}Nd [9] and a contamination of ^{208}Tl and ^{214}Bi in the detector dominates the background. The SuperNEMO group has developed the BiPo-3 detector to mea-

*Corresponding author. E-mail address: ito.hiroshi@crystal.kobe-u.ac.jp (H. Ito).

sure the radioactive impurities with sensitivity less than 2 μBq/kg (90%CL) for ^{208}Tl and 140 μBq/kg (90%CL) for ^{214}Bi [10]. Therefore, the background of $0\nu\beta\beta$ decay is not only a contamination by the end point of continuous energy in an ordinary $2\nu\beta\beta$ decay process, but also the radiative impurities such as ^{238}U and ^{232}Th in the detector.

To estimate the radioactive impurities in the detector material, the XMASS group measured ^{210}Pb and ^{210}Po in the bulk of copper by using a commercial alpha-particle detector (Ultra-Lo 1800, XIA) [11]. The alpha detector has a good energy resolution (as explained in Sec. 3.2) and a mechanism to reduce the background by waveform analysis, and thus a sensitivity is $\sim 10^{-4}$ α/cm^2/hr. However, it has no position sensitivity. A sample such as a micro pattern gas detector board has not an uniform radioactive contamination. For example, the impurities might be contaminated to the electrodes in a pattern making process. Therefore, a position-sensitive alpha detector is required to select materials for the rare-event-search experiments.

This paper is organized as follows. The details of the alpha-particle detector, setup, low-α micro pixel chamber (μ-PIC), gas circulation system, electronics, and trigger data acquisition system are described in Sec. 2. The performance check that uses the alpha-particle source, a sample test, and background estimation are described in Sec. 3. The remaining background of the detector and future prospects are discussed in Sec. 4. Finally, the study is concluded in Sec. 5.

2. Alpha-particle imaging detector based on gaseous micro-TPC

A new alpha-particle detector was developed based on a gaseous micro-TPC upgraded from the NEWAGE-0.3a detector [12] which was used to search for dark matter from September, 2008 to January, 2013. The detector consisted of the micro-TPC using a low-α μ-PIC, a gas circulation system, and electronics, as shown in Fig.1. The TPC was enclosed in a stainless-vessel for the gas seal during the measurement.

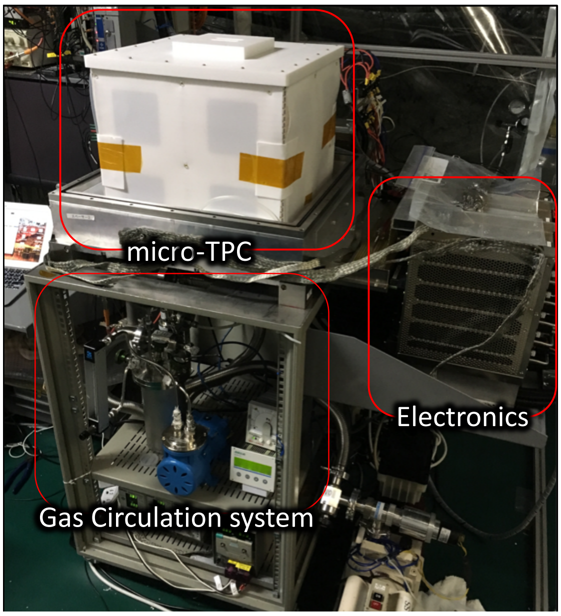

Fig. 1: Photographic of detector.

2.1. Setup and configuration

Figure 2 shows a schematic view of the detector, where the gas volume is $(35 \times 35) \times 31$ cm^3. The detector was placed underground at the Kamioka facility in Institute for Cosmic Ray Research, Japan. An oxygen-free copper plate with a surface polished to a roughness of 0.4 μm was used as the drift plate. The drift plate had an opening with a size of $(9.5 \times 9.5$ cm$^2)$ as a sample window. A copper mesh was set on the drift plate to hold the sample at the window area, as shown in Fig. 3. The electrons ionized by the alpha particles drift toward the μ-PIC with a vertical upward-pointing electric field E. CF_4 gas, which was also used in the NEWAGE-0.3a, was used as the chamber gas because of the low diffusion properties. The pressure was set at 0.2 bar as a result of the optimization between the expected track length and the detector stability. The track length was expected to be longer, which improved the tracking performance when the gas pressures was low, while the discharge rate of the μ-PIC increased. The electric field in the drift volume, $E = 0.4$ kV/cm/bar, was formed by supplying a negative voltage of 2.5 kV and placing field-shaping patterns with chain resistors every centimeter [13]. The drift velocity was 7.4 ± 0.1 cm/μs. The μ-PIC anode was connected to +550 V. The typical gas gain of μ-PIC was 10^3 at ~ 500 V.

2.2. Low-α μ-PIC

The background study for the direction-sensitive dark matter search suggests that μ-PIC has radiativoactive impurities of ^{238}U and ^{232}Th which emit

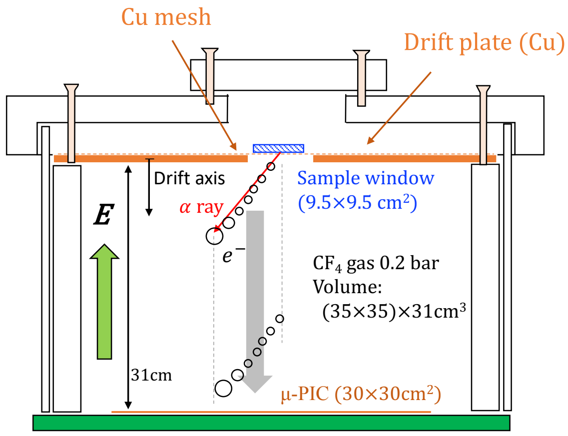

Fig. 2: Schematic cross section of detector setup.

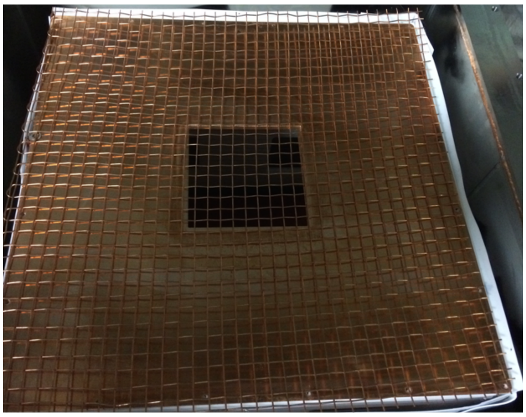

Fig. 3: Drift plate with a sample window (hole size is 9.5×9.5 cm^2) and copper support mesh.

alpha particles [5]. A survey with a HPGe detector revealed that μ-PIC's glass cloth was the main background source, and so the impurities were removed [14]. Details of the device with the new material, a low-α μ-PIC, will be described in Ref [15].

2.3. Gas circulation system

A gas circulation system that uses activated charcoal pellets was developed for radon-background suppression and to protect a against gain deterioration due to the outgassing. A pump (EMP, MX-808ST-S) and a needle-type circulate meter (KOFLOC, PK-1250) were used to flow the gas at a rate of ~ 500 cm^3/min. The gas pressure was monitored to ensure the stable operation of the circulation system and as maintained within an increase of $\sim 2\%$ for several weeks.

2.4. Electronics and trigger data acquisition system

The electronics for the μ-PIC readout consisted of amplifier-shaper discriminators [16] for 768 anode and 768 cathode signals and a position-encoding module [17] to reconstruct the hit pattern. A data acquisition system consisted of a memory board to record tracks and a flash analog-to-digital converter (ADC) for the energy measurement. The flash ADC with 100 MHz sampling recorded the sum signal of the cathode strips with a full time range of 12 μs. The anode sum signal issued the trigger. With this way of triggering, in contrast to the trigger by signal (for example, primary scintillation) in the TPC before the drift, the absolute position along the drift direction cannot be measured. However, because the alpha particles were expected to be emitted from the sample, the drift-along coordinate of the emission point was assumed to be the position of the drift plate.

3. Performance check

3.1. Alpha-particle source

A 10×10 cm^2 copper plate with ^{210}Pb accumulated on the surface was used as an alpha-particle source for the energy calibration and energy-resolution measurement [11]. The source emits alpha particles with an energy of 5.3 MeV as a decay of ^{210}Po. The alpha-particle emission rate (hereinafter called the α rate) of the source plate was calibrated to be 1.49 ± 0.01 α s^{-1} for 4.8–5.8 MeV by using the Ultra-Lo 1800 [11].

3.2. Energy calibration

An energy calibration was conducted with the alpha-particle source. The energy was calculated from the flash ADC waveform. Figure 4 shows a typical energy spectrum of the alpha-particle source. The energy resolution was estimated to be 6.7% (1σ) for 5.3 MeV, which is worse than the Ultra-Lo 1800 resolution of 4.7% (1σ) for 5.3 MeV. This deterioration was thought to be due to the gain variation of the μ-PIC detection area.

3.3. Event reconstruction

Figure 5 shows a typical event display with the tracks and flash ADC waveform data for alpha-particle emission from ^{210}Po. The hit points were determined based on coincidence of anode and cathode detections. Figure 5 (c) shows the anode-cathode plane for the track. The open circles are

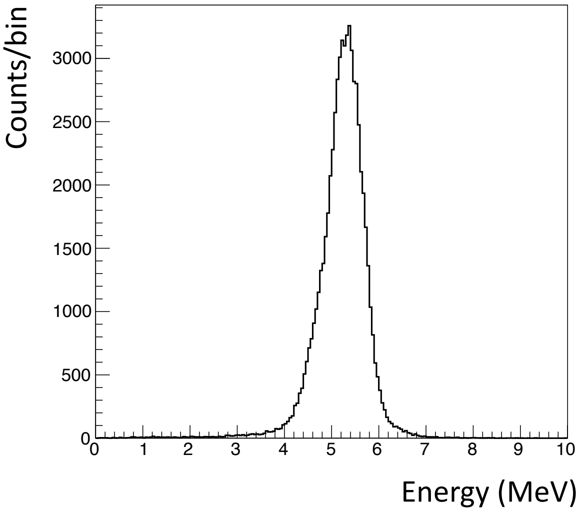

Fig. 4: Energy spectrum for alpha particles from ^{210}Po (5.3 MeV).

data. The red solid line is a linear fit result. The dashed line represents the edge of the sample window. The solid blue point is the emission point of the alpha particle. The scheme of the determination of the emission point, or the track sense, is explained in Sec. 3.4. Figure 5 (a) and (d) show anode- and cathode-drift planes, respectively. The drift coordinate is converted from the timing and is set to zero base, which corresponds to the drift-plate position. Figure 5 (b) shows a flash ADC waveform.

The track angles were determined on the anode-cathode, anode-drift, and cathode-drift planes. These angles were determined with a common fitting algorithm. First, the weighted means of the hit points $(x_{\rm w}, y_{\rm w})$ were defined as

$$\begin{pmatrix} x_{\rm w} \\ y_{\rm w} \end{pmatrix} = \frac{1}{n}\sum_{j=0}^{n}\begin{pmatrix} x_j \\ y_j \end{pmatrix}, \quad (1)$$

where x_j and y_j are the measured hit points and n is a number of points. Next, the track was shifted and rotated through the angle θ as follows

$$\begin{pmatrix} x'_j \\ y'_j \end{pmatrix} = \begin{pmatrix} \cos\theta & -\sin\theta \\ \sin\theta & \cos\theta \end{pmatrix}\begin{pmatrix} x_j - x_{\rm w} \\ y_j - y_{\rm w} \end{pmatrix}. \quad (2)$$

Here x'_j and y'_j are the points after the shift, and rotation and the angle θ were determined to minimize the quantity f, which is defined as

$$f(\theta) = \sum {y'}_j^2, \quad (3)$$

where this formula means a sum of the square of the distance between the rotated point and the x axis. This method has the advantage to determining the angle with no infinity pole at $\theta = 90°$, in contrast with a sample linear fit.

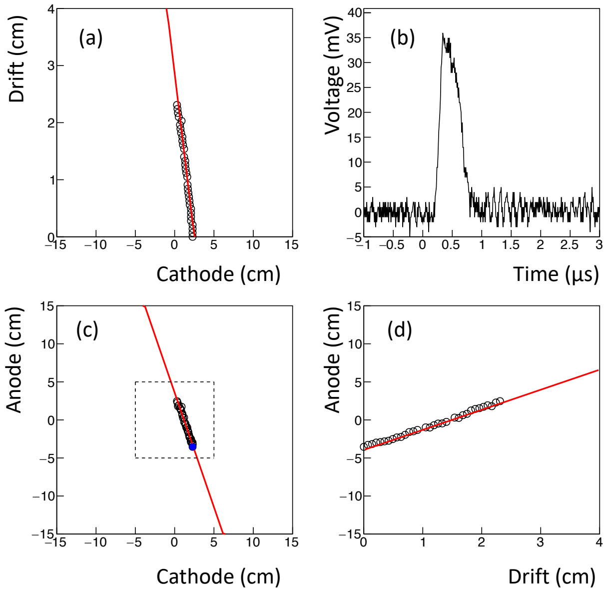

Fig. 5: Event display of an alpha particle from 210Po. (a) cathode-drift projection, (b) flash ADC waveform (c) cathode-anode projection, and (d) anode-drift projection are displayed. The drift coordinate is set to zero base corresponding to the drift plate position for the top of the track.

3.4. Track-sense determination

Backgrounds in low radioactivity alpha-particle detectors are in general alpha particles from the radon (radon-α) and material in the detector (detector-α). The radon-αs are expected to be distributed uniformly in the gas volume with isotropic directions. The detector-αs are expected to have position and direction distributions specific to their sources. One of the main sources of the detector-αs are the μ-PIC and the directions are mostly upward. Since the direction of alpha particles from the sample are downward, these detector-αs and half of the radon-αs can be rejected by the cut of upward-direction events.

The deposit energy per unit path length, dE/dx of an alpha particle with an initial energy over a few MeV, has a peak before stopping (Bragg peak). The number of electrons ionized by the alpha particle in the gas is proportional to dE/dx, and dE/dx along the track profile is projected onto the time evolution in the signal due to the mechanism of the TPC. This time profile was recorded as the waveform and thus the track sense (i.e., whether the tack was upward or downward) can be determined from the waveform.

A parameter to determine the track sense is

$$F_{\rm dwn} = S_2/(S_1 + S_2), \tag{4}$$

where S_1 and S_2 are the time-integrated waveform before and after the peak. They are defined as

$$S_1 = \int_{t_0}^{t_p} v(t)dt, \tag{5}$$

$$S_2 = \int_{t_p}^{t_1} v(t)dt. \tag{6}$$

Here, $t_0 = 0$ μs, $t_1 = 1.5$ μs, and t_p are the start, stop, and peak time, respectively, for the waveform shown in Fig. 5 (b). Figure 6 shows typical $F_{\rm dwn}$ distribution with the alpha-particle source, where most of the events are expected to be downward-oriented. The $F_{\rm dwn}$ values of the downward events are distributed around 0.7, as shown by the black-shaded histograms. Conversely, radon-αs have an isotropic direction, i.e., $F_{\rm dwn}$ has two peaks, as shown by the red solid histogram, where the radon-α are background events in the sample test data, as explained later. The scale of the source-α was normalized to the radon-α peak of downward for clarity. The selection efficiency of $F_{\rm dwn} > 0.5$ was estimated to be 0.964 ± 0.004 in the source-α spectrum while the radon background was reduced to half. The blue dashed histogram is a spectrum that subtracted the normalized source-α from the radon-α. The cut efficiency of the upward-oriented events ($F_{\rm dwn} \leq 0.5$) was estimated to be 0.85 ± 0.04. The energy dependence of $F_{\rm dwn}$ will be explained in Sec. 3.6.

3.5. Distribution of emission position

Since alpha particles are mainly emitted from the source, the top points of the alpha-particle tracks trace the shape of the radioactivity on the sample. Figures 7 (a) and 7 (b) show the anode–cathode projection distribution of the top and bottom of the alpha-particle tracks, respectively, where the top and bottom are defined as the zero and maximum drift coordinate, respectively, as shown in Figs. 5 (a) and 5 (d). The dashed line represents the edge of the drift-plate sample window. Comparing Fig. 7 (a) with Fig. 7 (b) clearly reveals the shape of the radioactivity.

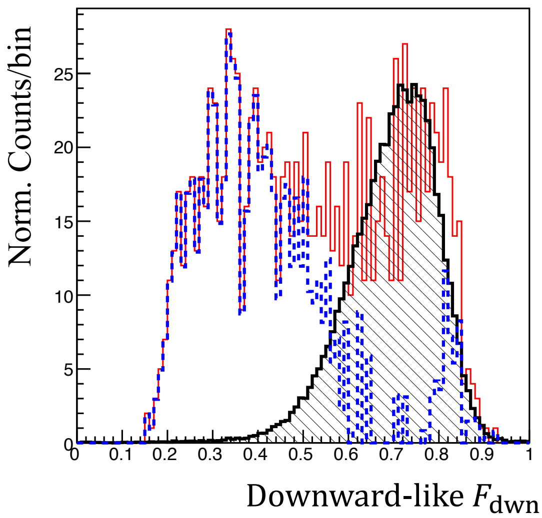

Fig. 6: Downward-oriented distribution for source-α (black shade), radon-α (red solid), and a histogram made by subtracting the radon-α spectrum from the source-α one(blue dashed).

The position resolution was evaluated along the four dashed lines in Fig. 7 (a). The number of events was projected onto the axis perpendicular to the lines and was fit with error functions. As a result, the position resolution was determined to be 0.68 ± 0.14 cm (σ), where the error is a standard deviation in the four positions.

3.6. Efficiency of event selection

3.7. Detection and selection efficiency

To select good events for alpha particles from the sample, we use the following criteria: (C1) selection for events with good fitting tracks, (C2) cut for the upward-oriented events, and (C3) selection for events with emission points in the sample region.

For criterion C1, the good fit to track events was selected as $f_{\rm min}(\theta)/(n-1) < 0.02$ cm^2 for the anode-cathode, anode-drift, and cathode-drift planes to remove events that had any noise and to remove candidates for electron tracks, where $f_{\rm min}(\theta)$ is a minimum of Eq. (3).

Criterion C2 rejects the upward-oriented tracks with > 3.5 MeV and $F_{\rm dwn} \leq 0.5$ because the determination efficiency depends on the energy. The upward- and downward-oriented tracks can be determined with 95% or more certainly at over 3.5 MeV. Note that this cut was applied for the events > 3.5 MeV, because the radon background, which was assumed to be the dominant background

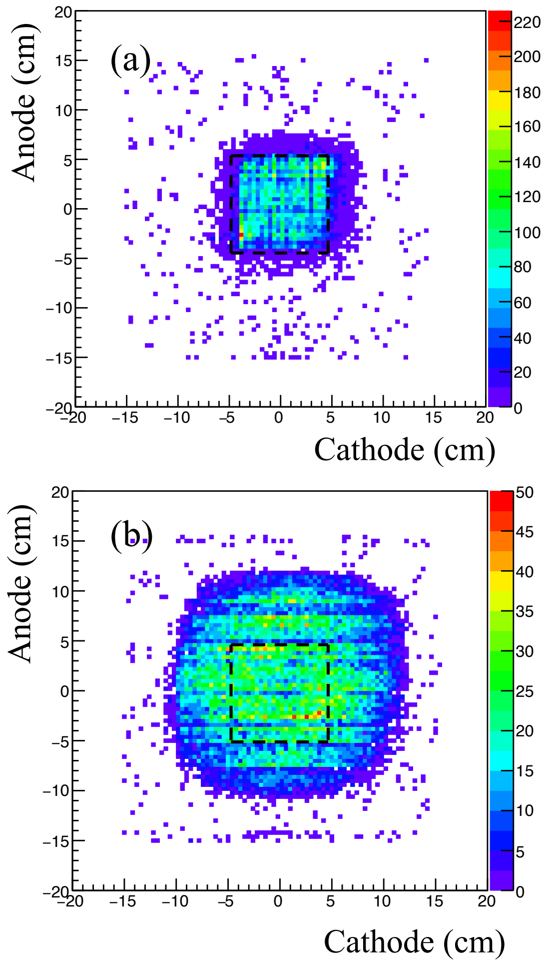

Fig. 7: Anode–cathode projection distributions of (a) top and (b) bottom of tracks for alpha particles emitted from the source. The dashed line is the edge of the sample window.

source, created the peak around 6 MeV and the contribution to the energy range below 3.5 MeV was limited.

For criterion C3, as shown in Fig. 7 (a), to reject the remained the radon and detector-αs, the selection region for alpha-particle emission point was set between -8.0 cm and 8.0 cm in both the anode and cathode coordinate. The rate of radon-α in the selected region was less than a few hundred time of source-α, and thus the it was a negligible.

The selection efficiency for C1, C2, and C3 containing the detection efficiency was $(2.17 \pm 0.29) \times 10^{-1}$ counts/α (the ratio of the count rate to the α rate of the source), where the error represents the systematic error of C1 to C3 selections and uncertainly of the source radioactivity and the statistic error is negligible.

3.8. Sample test and background estimate

3.8.1. Setup

A 5×5 cm^2 piece of the standard μ-PIC whose α rate was known to be 0.28 ± 0.12 α/cm^2/hr in previous work [14] served as a sample and was inspected by using the detector. The setup is shown in Fig. 8. The live time was 75.85 hr.

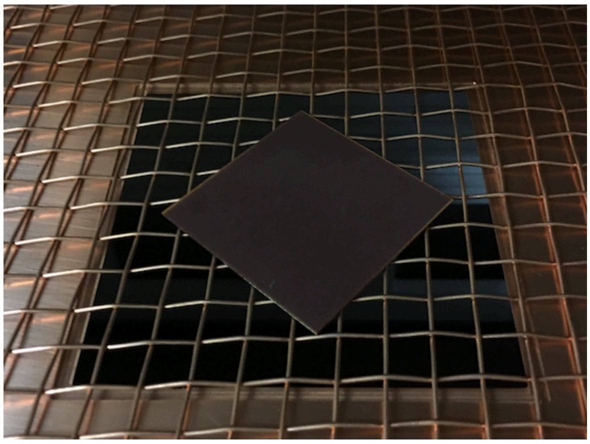

Fig. 8: Setup for a 5×5 cm^2 piece of the standard μ-PIC as sample.

3.8.2. Background in sample region

The α rate of the sample was estimated by subtracting the background rate. Considered background was mainly the radon-α. The detector measured both the α rates on the region of the sample and around the sample (outer region). The background rate could be determined from the α rate in the outer region. The net α rate from the sample was thus evaluated by subtracting the background rate from the rate of the sample region. It was necessary to confirm that the background rates in both regions were consistent with each other.

We checked the upward-oriented ($F_{\rm dwn} \leq 0.5$) α rate in both regions because the alpha particles from a sample are typically emitted downward. Measured energy spectra are shown in Fig. 9. The red- and black-shaded histograms show the energy spectra inside and outside the sample region, respectively. These spectra are scaled by the selection efficiency. Both peaks are around 6 MeV and α rates are $(2.16^{+0.54}_{-0.35}) \times 10^{-2}$ (inside) and $(1.54^{+0.64}_{-0.40}) \times 10^{-2}$ α/cm^2/hr (outside). Therefore, the background condition inside the sample region is consistent with the background condition outside the sample region. The alpha-particle energy spectrum is interpreted as the radon peaks at 5.5 MeV (^{222}Rn), 6.0 MeV (^{218}Po), and 7.7 MeV (^{214}Po).

The downward-oriented ($F_{\mathrm{dwn}} > 0.5$) α rate outside the sample is $(1.58^{+0.29}_{-0.26}) \times 10^{-2}$ α/cm^2/hr, as shown in the black-shaded spectrum of Fig. 11. In this work, the background rate was improved by one order of magnitude in comparison with that of our previous work [14]. The background reduction is attributed to the track-sense determination to reject upward-oriented alpha (for > 3.5 MeV) and the replacement of the low-α μ-PIC (for ≤ 3.5 MeV). In the energy region between 2.0 and 4.0 MeV, where most radon background is suppressed, the background rate is $(9.6^{+7.9}_{-5.6}) \times 10^{-4}$ α/cm^2/hr.

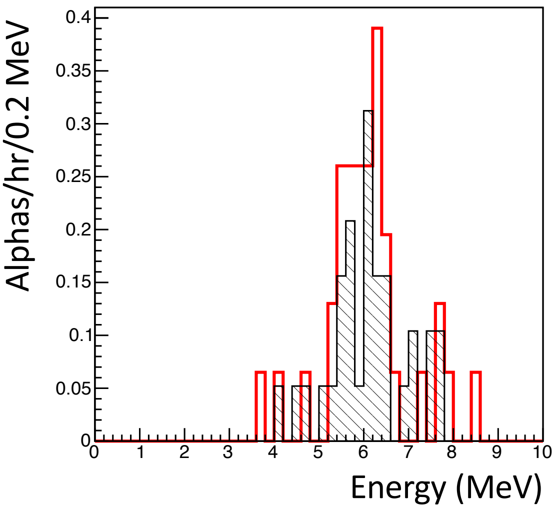

Fig. 9: Downward-oriented alpha-particle energy spectra inside (red) and outside (black shade) the sample region.

3.8.3. α rate of sample

Figure 10 shows the distribution of the top of the tracks for the sample, where the candidates are selected by the criteria C1 and C2. The regions ① and ② are sample and background regions, respectively. The sample region is the inside of ± 5 cm of anode and cathode. The background region is the outside of the sample region and the inside of ± 7.5 cm of anode and cathode. Figure 11 shows the energy spectra of downward-oriented alpha particles in the sample (red) and the background region (black shaded). The α rate of the sample was calculated to be $(3.57^{+0.35}_{-0.33}) \times 10^{-1}$ α/cm^2/hr (> 2.0 MeV) by subtracting the background rate.

Assuming the alpha spectrum is constituted only from ^{232}Th or ^{238}U, the impurity is estimated to be 6.0 ± 1.4 or 3.0 ± 0.7 ppm, respectively. The impurities of ^{232}Th and ^{238}U are measured to be 5.84 ± 0.03 and 2.31 ± 0.02 ppm, respectively, by using the HPGe detector. Although the error is huge because of the continuous energy spectrum, it is consistent with the prediction of prior measurement. In this sample test, it was demonstrated to observe the background alphas at the same time.

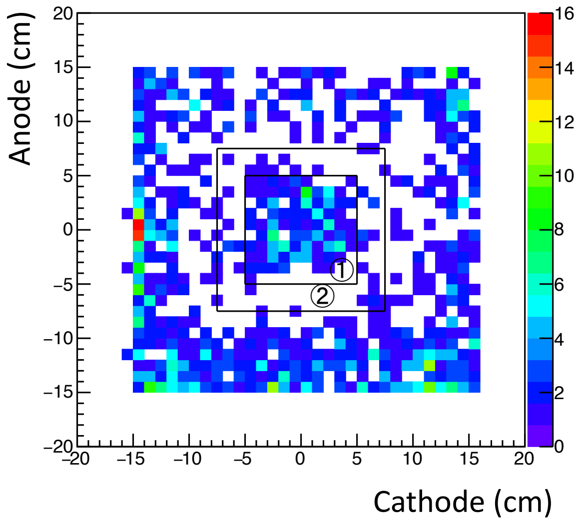

Fig. 10: Distribution of the top of downward-oriented alpha-particle track. The regions ① and ② are the sample and background regions, respectively.

4. Discussion

We begin by discussing the sensitivity for the energy between 2 and 9 MeV based on long-term measurements. In this energy range, the background is dominated by the radon-αs with $\sim (1.58^{+0.29}_{-0.26}) \times 10^{-2}$ α/cm^2/hr. The statistical error (σ) is expected to scale with the inverse of the square root of the measurement time (t) given as $\sigma \propto 1/\sqrt{t}$. In this work, the live time was only three days, and the statistical error was $\sigma \sim 3 \times 10^{-3}$. With a measurement time of one month, the error of radon-αs was estimated to be $\sigma \sim 1 \times 10^{-3}$ α/cm^2/hr. When the α rate as the same of the radon-αs was observed, the sum of squares of these σs for the sample and radon-αs would be expected to be a few 10^{-3} α/cm^2/hr as the measurement limit by subtraction with these α rates.

The edges region (anode $\sim \pm 15$ cm or cathode $\sim \pm 15$ cm) has a high rate of background, as shown

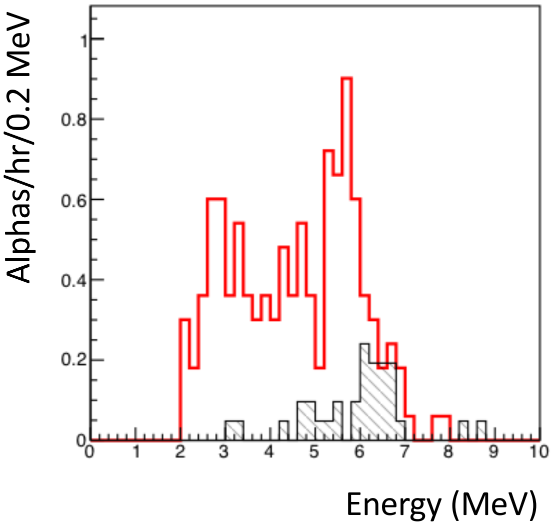

Fig. 11: Downward-oriented alpha-particle energy spectra in sample region (red) and background region (black shade).

in Fig. 10. These events have an energy and path-length dependence similar to that of the alpha particles. The alpha particles were mainly oriented upward and were emitted from outside the detection area. As an impurity candidate, a piece of the printed circuit board (PCB) was inspected and the α rate was $(1.16 \pm 0.06) \times 10^{-1}$ $\alpha/\mathrm{cm}^2/\mathrm{hr}$. Although the alpha-particle events could be rejected by the fiducial region cut, these impurities could be the radon sources (see Fig. 12). Therefore, as a next improvement, a material with less radiative impurities should be used for the PCB.

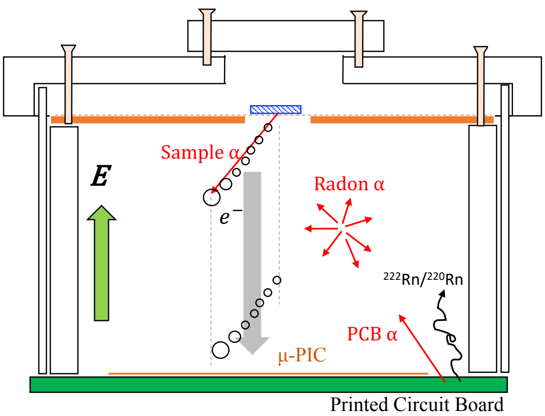

Fig. 12: Schematic cross section of background alpha particles in detector setup.

The goal for detector sensitivity is less than 10^{-4} $\alpha/\mathrm{cm}^2/\mathrm{hr}$, which corresponds to measuring radioactive impurities at the ppb level. We can potentially improve the background rate by using the cooled charcoal and using a material with less impurities. A recent study reported that a cooled charcoal could suppress the radon by 99% in the argon gas [18]. A recent NEWAGE detector suppresses the radon to 1/50 by using cooled charcoal [5]. With these improvements, the detector would achieved to the goal of performance.

5. Conclusion

We developed a new alpha-particle imaging detector based on the gaseous micro-TPC. The measured energy resolution is 6.7% (σ) for 5.3 MeV alpha particles. The measured position resolution is 0.68 ± 0.14 cm. Based on a waveform analysis, the downward-oriented events' selection efficiency is 0.964 ± 0.004 and the cut efficiency of the upward-oriented events is 0.85 ± 0.04 at > 3.5 MeV. Also, a piece of the standard μ-PIC was measured as a sample, and the result is consistent with the one by another measurement. A measurement of the alpha particles from a sample and background was also established at the same time. A background rate near the radon-α $((1.58^{+0.51}_{-0.42}) \times 10^{-2}$ $\alpha/\mathrm{cm}^2/\mathrm{hr})$ was achieved.

Acknowledgments

This work was supported by a Grant-in-Aid for Scientific Research on Innovative Areas, 26104004 and 26104008, from the Japan Society for the Promotion of Science in Japan. This work was supported by the joint research program of the Institute for Cosmic Ray Research (ICRR), the University of Tokyo. We thank Dr. Y. Nakano of the ICRR, University of Tokyo, Japan for providing us with a helium-gas leak detector.

References

[1] R Bernabei, et al., J. Phys. Conf. Ser. **1056** (2018) 012005.
[2] XENON Collaboration, Eur. Phys. J. **77** 881 (2017).
[3] D. S. Akerib, et al., Phys. Rev. Lett. **118** 021303 (2017).
[4] T. Tanimori, et al., Phys. Lett. B **578** (2004) 241.
[5] K. Nakamura, et al., Prog. Theo. Exp. Phys. (2015) 043F01.
[6] The GERDA Collaboration, Nature **544** (2017) 47.
[7] K.Asakura, et al., Nucl. Phys. A **946** (2016) 171.
[8] R. Arnold, et al., Eur. Phys. J. C **78** (2018) 821.

[9] R. Arnold, et al., PRL **119**, 041801 (2017).
[10] A. S. Barabash, et al., JINST **12** (2017) P06002.
[11] K. Abe, et al., Nucl. Instr. Meth. A **884** (2018) 157.
[12] K. Miuchi, et al., Phys. Lett. B **686** (2010).
[13] K. Miuchi, et al., Phys. Lett. B **654** (2007) 58.
[14] T. Hashimoto, et al., AIP Conf. Proc. **1921**, 070001 (2018).
[15] T. Hashimoto, et al., in preparation.
[16] R. Orito, et al., IEEE Trans. Nucl. Scie. **51**, 4 (2004) 1337.
[17] H. Kubo, et al., Nucl. Instr. Meth. A **513** (2003) 93.
[18] M. Ikeda, et al., Radioisotopes, **59**, (2010) 29.